



Heterogeneous CO₂ and CH₄ patterns across space and time in a small boreal lake

Blaize A. Denfeld , Anna Lupon , Ryan A. Sponseller , Hjalmar Laudon & Jan Karlsson

To cite this article: Blaize A. Denfeld , Anna Lupon , Ryan A. Sponseller , Hjalmar Laudon & Jan Karlsson (2020) Heterogeneous CO₂ and CH₄ patterns across space and time in a small boreal lake, Inland Waters, 10:3, 348-359, DOI: [10.1080/20442041.2020.1787765](https://doi.org/10.1080/20442041.2020.1787765)

To link to this article: <https://doi.org/10.1080/20442041.2020.1787765>



© 2020 The Author(s). Published by Informa UK Limited, trading as Taylor & Francis Group



[View supplementary material](#)



Published online: 03 Sep 2020.



[Submit your article to this journal](#)



Article views: 246



[View related articles](#)



[View Crossmark data](#)

Heterogeneous CO₂ and CH₄ patterns across space and time in a small boreal lake

Blaize A. Denfeld ^a, Anna Lupon,^b Ryan A. Sponseller,^a Hjalmar Laudon,^c and Jan Karlsson^d

^aDepartment of Ecology and Environmental Science, Umeå University, Umeå, Sweden is Linnaeus väg 4-6, 907 36 Umeå; ^bIntegrative Freshwater Ecology Group, Center for Advanced Studies of Blanes (CEAB-CSIC), Blanes, Spain; ^cDepartment of Forest Ecology and Management, Swedish University of Agricultural Sciences, Umeå, Sweden; ^dClimate Impacts Research Centre, Department of Ecology and Environmental Science, Umeå University, Umeå, Sweden

ABSTRACT

Small boreal lakes emit large amounts of carbon dioxide (CO₂) and methane (CH₄) to the atmosphere. Yet emissions of these greenhouse gases are variable in space and time, in part due to variable within-lake CO₂ and CH₄ concentrations. To determine the extent and the underlying drivers of this variation, we measured lake water CO₂ and CH₄ concentrations and estimated associated emissions using spatially discrete water samples collected every 2 weeks from a small boreal lake. On select dates, we also collected groundwater samples from the surrounding catchment. On average, groundwater draining a connected peat mire complex had significantly higher CO₂ and CH₄ concentrations compared to waters draining forest on mineral soils. However, within the lake, only CH₄ concentrations nearshore from the mire complex were significantly elevated. We observed little spatial variability in surface water CO₂; however, bottom water CO₂ in the pelagic zone was significantly higher than bottom waters at nearshore locations. Overall, temperature, precipitation, and thermal stratification explained temporal patterns of CO₂ concentration, whereas hydrology (discharge and precipitation) best predicted the variation in CH₄ concentration. Consistent with these different controls, the highest CO₂ emission was related to lake turnover at the end of August while the highest CH₄ emission was associated with precipitation events at the end of June. These results suggest that annual carbon emissions from small boreal lakes are influenced by temporal variation in weather conditions that regulate thermal stratification and trigger hydrologic land–water connections that supply gases from catchment soils to the lake.

ARTICLE HISTORY

Received 7 October 2019
Accepted 22 June 2020

KEYWORDS

carbon dioxide; carbon emissions; groundwater; lakes; methane; mire


Introduction

Small boreal lakes are globally abundant (Verpoorter et al. 2014) and, despite their small surface area, emit a significant amount of carbon dioxide (CO₂) and methane (CH₄) to the atmosphere (Tranvik et al. 2009, Bastviken et al. 2011). Emissions of these important greenhouse gases are, in part, dependent on within-lake CO₂ and CH₄ supply, which can be high in small boreal lakes (Kortelainen et al. 2006, Juutinen et al. 2009). Concentrations of CO₂ and CH₄ in lakes are governed by internal biogeochemical processes (e.g., organic matter decomposition, methanogenesis, respiration, primary production, and methane oxidation) as well as external inputs from the surrounding catchment (Cole et al. 2007). These internal and external controls can be highly dynamic and result in large spatial (Hofmann 2013, Schilder et al. 2013, Natchimuthu et al. 2016, 2017) and seasonal (Kortelainen et al. 2006, Juutinen et al.

2009, Karlsson et al. 2013, Vachon et al. 2017b) variability in CO₂ and CH₄ concentrations and emissions within a given lake. Further, spatiotemporal patterns between CO₂ and CH₄ may differ (e.g., Riera et al. 1999, Natchimuthu et al. 2014, Bartosiewicz et al. 2015, Loken et al. 2019) because important distinctions exist between the gases. For example, internal CO₂ production via organic matter decomposition occurs in aerobic and anaerobic environments, whereas CH₄ production is exclusively carried out under anaerobic conditions. Yet, historically CO₂ and CH₄ emissions have most often been measured separately, based on samples collected in the pelagic zone during summer, and thus neglect spatiotemporal variation in gas concentrations (e.g., Klaus et al. 2019).

Complexity in the internal and external controls on CO₂ and CH₄ has made predicting within-lake variation in CO₂ and CH₄ concentrations a challenge. Internal production and consumption of both carbon (C) gases

CONTACT Blaize A. Denfeld  bdenfeld@gmail.com,  Now at ICF, 1800 G St. NW, Washington, DC, 20006, USA

 Supplemental data for this article can be accessed here <https://doi.org/10.1080/20442041.2020.1787765>.

© 2020 The Author(s). Published by Informa UK Limited, trading as Taylor & Francis Group

This is an Open Access article distributed under the terms of the Creative Commons Attribution-NonCommercial-NoDerivatives License (<http://creativecommons.org/licenses/by-nc-nd/4.0/>), which permits non-commercial re-use, distribution, and reproduction in any medium, provided the original work is properly cited, and is not altered, transformed, or built upon in any way.

respond to shared drivers of sediment and water characteristics such as nutrients, dissolved organic matter (DOM), oxygen availability, and temperature. Despite this, heterogeneous biogeochemical properties within and among lakes, as well as differences in production and consumption processes between C gases, can result in distinct underlying drivers for spatial patterns in CO₂ and CH₄. For example, some authors have observed highest CO₂ concentrations in the stratified pelagic (central) zone (Schilder et al. 2013) while others have reported peaks in the littoral (nearshore) zone, near stream inlets rich in CO₂ (Natchimuthu et al. 2017). By comparison, concentrations of CH₄ are generally higher in littoral than in pelagic zones (Hofmann 2013, Schilder et al. 2013, Encinas Fernández et al. 2016, Natchimuthu et al. 2016), which is attributed to elevated diffusion and ebullition in warm, near-shore sediments (Bastviken et al. 2008, DelSontro et al. 2016), the presence of macrophytes (Juutinen et al. 2003, Wang et al. 2006), and CH₄-rich inflow from streams and groundwater (Striegl and Michmerhuizen 1998, Murase et al. 2003). The role of external inputs is likely to be particularly important for spatial gas dynamics in many small lakes, where generally shorter water residence time and high drainage ratios strengthen the influence of external inputs of CO₂ and CH₄ (Vachon et al. 2017a).

In addition to within-lake spatial variability, CO₂ and CH₄ concentrations and emissions in boreal lakes also fluctuate seasonally, often with the highest emissions occurring during mixing events following ice-melt in the spring and the breakdown of summer stratification in autumn (Riera et al. 1999, López Bellido et al. 2009). However, smaller mixing events (e.g., upwelling from oscillating internal waves, intrusions from rainfall) may also occur throughout the open water period (Bartosiewicz et al. 2015) and can lead to occasionally high, but variable, CO₂ and CH₄ emissions (e.g., Natchimuthu et al. 2017). Thus, changes in thermal dynamics within the epilimnion can be important in determining surface water C gas variation (Åberg et al. 2010). Finally, precipitation can impact within-lake CO₂ and CH₄ concentrations by enhancing organic matter and gas inputs to lakes via runoff (Rantakari and Kortelainen 2005, Ojala et al. 2011, Vachon and del Giorgio 2014). Because changes in weather conditions, including temperature and precipitation, are episodic and often unpredictable (Jennings et al. 2012), the short-term response of CO₂ and CH₄ variations is commonly missed in seasonal emission estimates. Given that the frequency of extreme weather events will likely increase in the future (Hartmann et al. 2013), it is important that we capture how these events influence within-lake dynamics of C gases at a suitable temporal scale.

In this study, we evaluated the patterns and drivers of CO₂ and CH₄ concentrations and emissions in a small boreal lake throughout the open water period. We explored these spatiotemporal patterns in a lake composed of 2 distinct subbasins, one surrounded by a mire complex dominated by organic peat soils and the other primarily fed by water originating from forest on mineral soils. We hypothesized that these different catchment waters sources would shape the spatial and temporal patterns of CO₂ and CH₄ concentrations. Accordingly, we expected to find the highest gas concentrations in littoral zones bordering the mire complex because mires are important sources of CO₂ and CH₄ to boreal running waters (Dinsmore et al. 2010, Leach et al. 2016). We further predicted that the CH₄:CO₂ ratio in littoral zones would be elevated because of increased CH₄ diffusion and ebullition in warm, near-shore sediments (Bastviken et al. 2008). Furthermore, given the importance of the mire complex and the small size of the study lake, we expected that hydrological inputs would be more important than temperature and lake stratification in explaining temporal variation in lake CO₂ and CH₄ dynamics. To test these predictions, we measured aqueous CO₂ and CH₄ concentrations from spatially discrete locations in the lake every 2 weeks and from surrounding catchment groundwater on select dates. We then related within-lake CO₂ and CH₄ concentrations to temperature, hydrology, and lake thermal stratification and calculated average CO₂ and CH₄ emissions for each sampling date.

Methods

Study lake

Lake Stortjärn is a low productivity, small (0.04 km²) lake located in the Krycklan Research Catchment in northern boreal Sweden (64°15'N, 19°45'E), with a maximum depth of 6.7 m, mean depth of 2.7 m, and catchment area of 0.65 km² (Fig. 1). The lake is divided into 2 distinct subbasins; water enters the lake via a small inlet ditch stream and mainly coniferous forest (*Pinus sylvestris*, *Picea abies*, and *Betula pubescens*) growing on mineral soil in the eastern subbasin, and via a *Sphagnum* peat moss mire complex in the western subbasin (Laudon et al. 2013). Water exits the lake via an outlet stream in the western subbasin. During the 2016 study year, the lake was ice-free at the end of May and was ice-covered again by the end of October. Thus, the open water period lasted less than 6 months, comparable to the lake water residence time of 5.6 months (approximately the lake volume/annual average discharge in 2016). Over the sampling period in 2016,

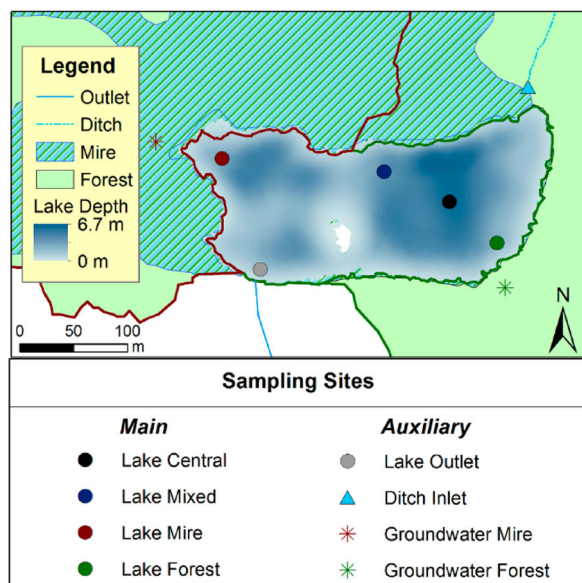


Figure 1. Lake Stortjärn (64°15'N, 19°45'E), a small boreal lake. The lake has 2 distinct subbasins, draining a mire complex in the western subbasin (brown border) and mainly forest in the eastern subbasin (green border). Water samples were collected from the lake and surrounding catchment. Surface and bottom waters were sampled at the 4 main lake sites. Only surface water was sampled at the Lake Outlet and Inlet Ditch sites. (Color version can be viewed online.)

mean (standard deviation) annual air temperature was 10 (5) °C and total precipitation was 278 mm, measured as part of the reference climate monitoring program at Svartberget experimental forest (Vindeln, Sweden).

Water sampling

From 31 May to 18 October 2016, we sampled the lake every 2 weeks (11 dates). We had 4 main lake sampling sites: 3 in littoral zones that bordered the mire complex, forest, and a mire–forest mixed zone, respectively (named L_{Mire} , L_{Forest} and L_{Mixed} hereafter), and 1 in the pelagic central zone of the lake (named L_{Central} hereafter; Fig. 1). The L_{Central} site, in the eastern subbasin, corresponds to the Swedish Infrastructure for Ecosystem Science (SITES) Water routine lake monitoring location (<http://www.fieldsites.se>). On each sampling date, we collected lake water from the surface (at 0.5 m depth) and bottom (at 2 m depth for all sites, except L_{Central} sampled at 4 m depth) at the 4 main lake sites. Surface and bottom water samples represented the epilimnion and hypolimnion layer, respectively, during stratification periods (Supplemental Fig. S1). At these sites, bottom water dissolved oxygen was also recorded (D-Opto, Zebra-Tech Ltd, New Zealand). In addition, we collected surface water at the lake shore near the outlet stream (named L_{Outlet} hereafter).

During the same time period on selected sampling dates we used a peristaltic pump to sample groundwater

from wells installed in the forest and mire subbasins of the catchment (named C_{Mire} and C_{Forest} hereafter) and also manually collected surface water samples from the inlet ditch stream (named C_{Inlet} hereafter; Fig. 1). Groundwater wells were installed to 110 cm and were screened from 5–105 cm; thus, these samples represent a depth-integrated estimate of dissolved C gases in the groundwater.

We analyzed all water samples for CO_2 and CH_4 concentration. Briefly, in the field we collected 5 mL of bubble-free water with a syringe and immediately injected the water into a 22.5 mL glass vial containing nitrogen gas (N_2) at atmospheric pressure and sealed it with a bromobutyl rubber septa (e.g., Wallin et al. 2010). The vials were prefilled with 0.5 mL of 0.6% HCl to shift the carbonate equilibrium toward free CO_2 (i.e., essentially all dissolved inorganic carbon [DIC] was transformed to CO_2). Within a week, headspace partial pressure of CO_2 and CH_4 were analyzed on a gas chromatograph equipped with a flame ionization detector (Perkin Elmer Autosystem Gas chromatograph, Waltham, MA, USA) and methanizer operating at 375 °C. Separation was carried out on a Hayesep N column using N_2 (40 mL per min) as the carrier gas. CH_4 concentration was calculated according to Henry's law, correcting for in situ temperature (Wiesenburg and Guinasso 1979). CO_2 concentration was calculated from DIC using temperature-dependent equations for the carbonate equilibrium (Gelbrecht et al. 1998) and Henry's Law (Weiss 1974) together with in situ pH and temperature. In the lab, pH was immediately analyzed using an Orion 9272 pH meter (DIC and pH values are reported in Supplemental Table S1).

For lake water, we denoted the C gas concentration in the surface water as $\text{CO}_{2\text{SW}}$ and $\text{CH}_{4\text{SW}}$ and in the bottom water as $\text{CO}_{2\text{BW}}$ and $\text{CH}_{4\text{BW}}$. Water collected from the surrounding catchment, groundwater wells, and the ditch was denoted as $\text{CO}_{2\text{CW}}$ and $\text{CH}_{4\text{CW}}$. As an index of anaerobic processes (Stanley et al. 2016), we also calculated the ratio of CH_4 to CO_2 in lake surface ($\text{CH}_4:\text{CO}_{2\text{SW}}$) and bottom waters ($\text{CH}_4:\text{CO}_{2\text{BW}}$) as well as in catchment water samples ($\text{CH}_4:\text{CO}_{2\text{CW}}$).

Monitoring data

We collected monitoring data on lake temperature, lake outlet discharge, and meteorological conditions over the entire sampling period. At the 4 main lake sites we deployed thermistor strings equipped with temperature loggers (Hobo TidbiT V2, Onset Inc., Bourne, MA, USA) every 0.2 m in the top 1 m and then every 0.5 m to the bottom to monitor water temperature

every 10 min throughout the water column. Using the temperature profile data, we calculated the lake stratification strength, as measured by Brunt-Vaisala buoyancy frequency ($\text{Strat}_{\text{Buoy}}$), using the *buoyancy.freq* function, provided by the *rLakeAnalyzer* package in R (Read et al. 2011). Meteorological data, including atmospheric temperature ($^{\circ}\text{C}$), precipitation (mm), wind speed (m s^{-1}), global radiation (W m^{-2}), and relative humidity, were obtained from a tower located 2 km from the lake in the Svartberget experimental forest ($64^{\circ}15'\text{N}$, $19^{\circ}46'\text{E}$). Wind speed was measured at 32 m height and adjusted to a height of 10 m following Crusius and Wanninkhof (2003). We averaged all data to hourly and daily means. For each sampling date, we calculated the antecedent average air temperature (Temp_{Ant}), total precipitation (Prec_{Ant}), and average wind speed (Wind_{Ant}) for the 2 weeks prior to the sampling date. Additionally, we obtained daily lake outlet discharge (Q_{OUT} , L s^{-1}) from the Krycklan routine monitoring program (Site C5; Laudon et al. 2013, Karlsten et al. 2016). Q_{OUT} represents the lagged response of the lake to precipitation events, that is, rainwater laterally transported from the catchment to the lake is not immediately flushed downstream (Supplemental Fig. S2).

CO₂ and CH₄ emission

For each sampling date, we calculated an average CO_2 and CH_4 emission (named $\text{CO}_{2\text{EM}}$ and $\text{CH}_{4\text{EM}}$ hereafter; $\text{mmol m}^{-2} \text{d}^{-1}$) for the 2 weeks prior to the sampling date. Emission was calculated using Fick's law of diffusion, where the gas exchange velocity (k) for the specific C gas was multiplied by the difference between the surface water concentration and the concentration in the atmosphere (acquired from www.wsrl.noaa.gov). For both gases, we set the concentration to the average derived from all 5 surface water lake sites. For comparison purposes, we also calculated emissions using gas concentrations only at the $\text{L}_{\text{Central}}$ site. Because we did not have direct measurements of k , we estimated a range of CO_2 and CH_4 emission rates from k_{600} using 2 different models calibrated for small lakes: a simple wind-speed derived model (Cole and Caraco 1998) and a boundary layer approach that considers wind shear and cooling (Heiskanen et al. 2014). Modeled k_{600} calculations were made using the *LakeMetabolizer* package in R (Winslow et al. 2016). Both models utilized wind speed adjusted to 10 m as an input variable, whereas the boundary layer approach utilized additional variables including latitude, lake area, air pressure, air temperature, relative humidity, longwave radiation, surface water temperature, depth of the

actively mixed layer, and light extinction coefficient. We calculated net longwave radiation and the depth of the actively mixed layer, following Read et al. (2011), and light extinction coefficient, according to Staehr et al. (2012). To obtain k from k_{600} , we applied the Schmidt number parametrizations (Wanninkhof 1992) using the temperature-dependent Schmidt number for CO_2 and CH_4 (600 at 20°C) following Jähne et al. (1987) and assuming a Schmidt number coefficient of -0.67 . We computed total emission estimates (mmol m^{-2}) for each 2-week sampling period by multiplying the $\text{CO}_{2\text{EM}}$ and $\text{CH}_{4\text{EM}}$ by 13 days.

Statistics

To test for differences in CO_2 and CH_4 concentrations among sampling sites we used a one-way analysis of variance (ANOVA). We normalized C gas concentrations to remove temporal variation from the data by dividing concentrations by the respective mean concentration of the sampling date. In total, we ran 6 separate ANOVA tests to examine spatial differences in $\text{CO}_{2\text{SW}}$, $\text{CO}_{2\text{BW}}$, $\text{CH}_{4\text{SW}}$, $\text{CH}_{4\text{BW}}$, $\text{CH}_4:\text{CO}_{2\text{SW}}$, and $\text{CH}_4:\text{CO}_{2\text{BW}}$. Surface waters included all 5 lake sites, whereas bottom waters only included the 4 main lake sites. We used a post hoc Tukey's test to determine which sites were statistically different. In addition, we ran a Welch's *t*-test to compare gas concentration (i.e., $\text{CO}_{2\text{CW}}$ and $\text{CH}_{4\text{CW}}$) between water samples collected from the forest (C_{Forest} and C_{Inlet}) and mire (C_{Mire}) subbasins. In all cases, differences were considered statistically significant at $p < 0.05$. Finally, we used nonparametric Kendall's rank correlations between the average lake CO_2 and CH_4 concentration and Temp_{Ant} , Prec_{Ant} , Q_{Out} , and $\text{Strat}_{\text{Buoy}}$ to explore potential drivers of temporal patterns. Statistical calculations were carried out in R 3.4.2.

Results

Spatial CO₂ and CH₄ variation

Surface and bottom water CO_2 concentrations spanned 2 orders of magnitude (Fig. 2a, d), 42–121 and 49–397 μM for $\text{CO}_{2\text{SW}}$ and $\text{CO}_{2\text{BW}}$, respectively. $\text{CO}_{2\text{SW}}$ showed no spatial pattern (ANOVA: $F = 1.0$, $p > 0.05$), whereas $\text{CO}_{2\text{BW}}$ was statistically different among sites (ANOVA: $F = 11.0$, $p < 0.001$). $\text{CO}_{2\text{BW}}$ at the $\text{L}_{\text{Central}}$ site was higher than all 3 nearshore sites (Tukey's HSD: $p < 0.01$). Within-lake surface and bottom water CH_4 concentrations were also variable (Fig. 2b, e), 0.2–0.6 and 0.1–1.8 μM for $\text{CH}_{4\text{SW}}$ and

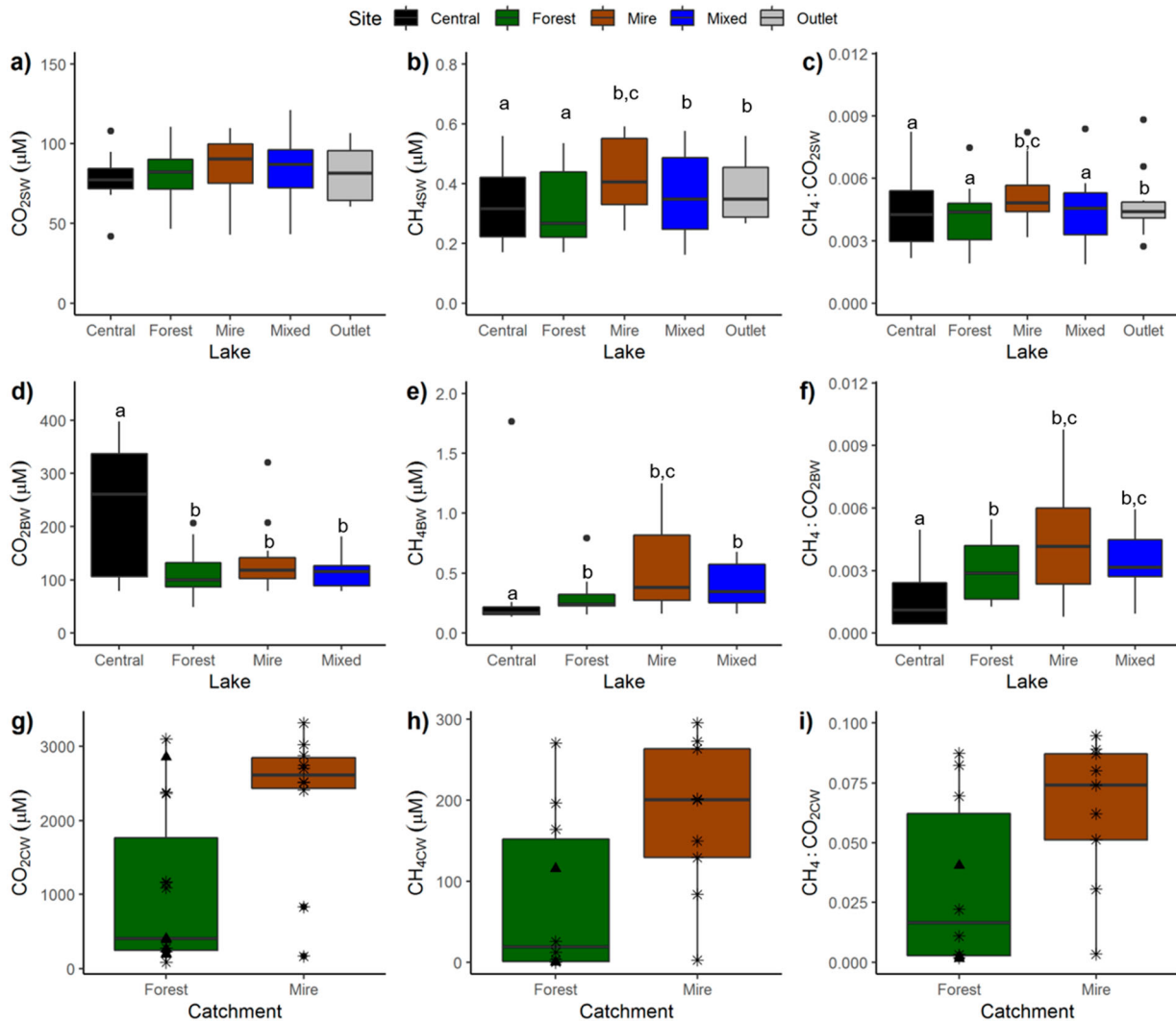


Figure 2. Spatial CO_2 , CH_4 , and $\text{CH}_4:\text{CO}_2$ gases concentrations in (a–c) lake surface and (d–f) bottom waters as well as (g–i) catchment waters sampled from groundwater wells (asterisk) and the ditch inlet (triangles). Boxes indicate the 25th percentile, median, and 75th percentile, and the whiskers extend to 1.5 times the interquartile range of the box. Letters indicate post hoc Tukey's test results (run on normalized data). (Color version can be viewed online.)

$\text{CH}_{4\text{BW}}$, respectively. Both $\text{CH}_{4\text{SW}}$ (ANOVA: $F = 5.01$, $p < 0.01$) and $\text{CH}_{4\text{BW}}$ (ANOVA: $F = 3.6$, $p < 0.05$) were statistically different among sites. $\text{CH}_{4\text{SW}}$ at the L_{Mire} site was significantly higher than $\text{CH}_{4\text{SW}}$ at the L_{Central} and L_{Forest} sites but not significantly different from the L_{Mixed} and L_{Outlet} sites (Tukey's HSD: $p < 0.05$). Similarly, $\text{CH}_{4\text{BW}}$ at the L_{Mire} nearshore site was only significantly higher than the L_{Central} site (Tukey's HSD: $p < 0.05$). The $\text{CH}_4:\text{CO}_2$ ratio (Fig. 2c, h) was also statistically different among sites in both surface ($\text{CH}_4:\text{CO}_{2\text{SW}}$: ANOVA: $F = 6.97$, $p < 0.001$) and bottom ($\text{CH}_4:\text{CO}_{2\text{BW}}$: ANOVA: $F = 5.9$, $p < 0.01$) waters. The L_{Mire} site had significantly higher $\text{CH}_4:\text{CO}_{2\text{SW}}$ than all other sites, except L_{Outlet} (Tukey's HSD: $p < 0.05$), whereas $\text{CH}_4:\text{CO}_{2\text{BW}}$ at the L_{Mire} and L_{Mixed} nearshore site was higher than at the L_{Central} site (Tukey's HSD: $p < 0.05$).

Generally, concentration of C gases in groundwater samples (Fig. 2g–i) were higher than in lake water samples. Maximum $\text{CO}_{2\text{CW}}$ (3315 μM) and $\text{CH}_{4\text{CW}}$ (295 μM) were 1 and 2 orders of magnitude higher than maximum lake water CO_2 and CH_4 , respectively. Finally, spatial patterns existed for catchment water samples. $\text{CO}_{2\text{CW}}$ (t -test: $t = 8.3$, $p < 0.05$) and $\text{CH}_{4\text{CW}}$ (t -test: $t = 4.7$, $p < 0.05$) in soil waters were significantly different between the 2 subbasins. The average $\text{CO}_{2\text{CW}}$ (2312 μM) and $\text{CH}_{4\text{CW}}$ (178 μM) was higher in the mire subbasin than the forest subbasin (1078 and 79 μM for $\text{CO}_{2\text{CW}}$ and $\text{CH}_{4\text{CW}}$, respectively).

Temporal CO_2 and CH_4 variation

Temporal patterns in lake CO_2 (Fig. 3a) and CH_4 (Fig. 3b) concentration corresponded to distinct periods

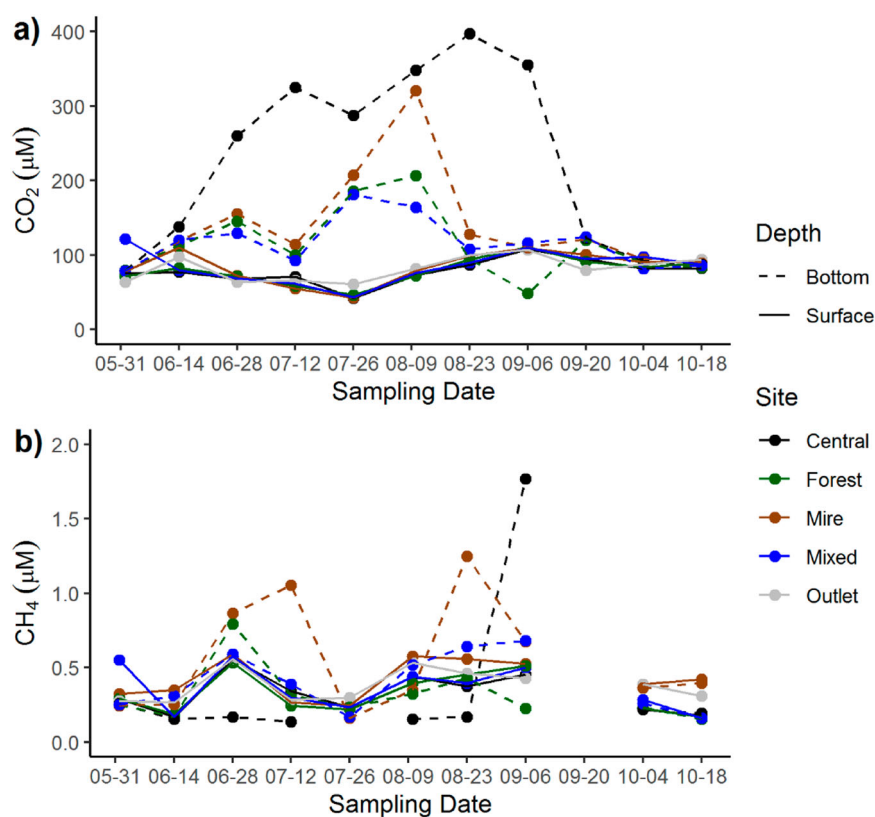


Figure 3. Temporal patterns in (a) CO_2 and (b) CH_4 concentrations in surface and bottom waters over the sampling period. CH_4 samples were compromised for the 20 September sampling.

in lake thermal structure (Fig. 4) and bottom water oxygen concentrations (Supplemental Fig. S3). Average $\text{CO}_{2\text{SW}}$ was elevated in early June ($81 \mu\text{M}$) and declined steadily (to $47 \mu\text{M}$) over the first 2 months of sampling. By the end of August, however, average $\text{CO}_{2\text{SW}}$ had doubled over the preceding month (Table 1) and continued to remain high through early September. In bottom

waters, average $\text{CO}_{2\text{BW}}$ increased from early June ($79 \mu\text{M}$) to early August ($260 \mu\text{M}$), mainly at the L_{Central} site, and decreased thereafter. By comparison, CH_4 concentrations were stochastic. Average $\text{CH}_{4\text{SW}}$ was elevated during the late June sampling ($0.56 \mu\text{M}$) and throughout August into September (0.45 – $0.48 \mu\text{M}$). Similarly, $\text{CH}_{4\text{BW}}$ accumulated at the end of June ($0.61 \mu\text{M}$) and again in late August and early September (0.62 and $0.84 \mu\text{M}$, respectively), particularly at the L_{Mire} site. From mid-September on, both CO_2 and CH_4 concentrations were homogeneous across the lake.

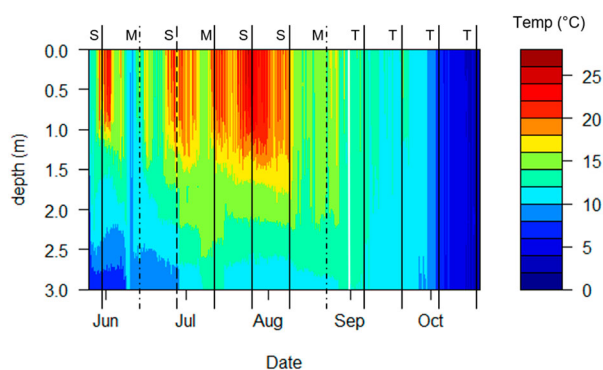


Figure 4. Water temperature with depth at the L_{Mire} site. Over the sampling period, the lake transitioned between stratified (S) and mixed (M) periods until complete turnover (T). Lines represent sampling dates with the peak $\text{CO}_{2\text{EM}}$ (dot dash) and $\text{CH}_{4\text{EM}}$ (long dash). The white line indicates a gap in the data, when loggers were removed for data download (see Supplemental Fig. S1 for temperature profiles at all 4 main lake sampling sites).

Drivers of CO_2 and CH_4 variation

Correlations between concentrations of C gases and explanatory variables (e.g., temperature, hydrology, lake stratification strength) suggested different temporal drivers for CO_2 and CH_4 (Table 2). In general, $\text{CO}_{2\text{SW}}$ and $\text{CO}_{2\text{BW}}$ correlated with $\text{Prec}_{\text{Antb}}$, $\text{Temp}_{\text{Antb}}$ and $\text{Strat}_{\text{Buoy}}$. However, $\text{CO}_{2\text{SW}}$ decreased with $\text{Prec}_{\text{Antb}}$, $\text{Temp}_{\text{Antb}}$ and $\text{Strat}_{\text{Buoy}}$, whereas $\text{CO}_{2\text{BW}}$ increased with these 3 explanatory variables. By contrast, CH_4 was only strongly correlated with hydrologic variables, with $\text{CH}_{4\text{SW}}$ positively correlated to Prec_{Ant} and Q_{Out} and $\text{CH}_{4\text{BW}}$ positively correlated only to Q_{Out} . Finally, $\text{CH}_4:\text{CO}_{2\text{SW}}$ and $\text{CH}_4:\text{CO}_{2\text{BW}}$ variations were positively correlated

Table 1. CO₂ and CH₄ surface (SW) and bottom water (BW) concentration mean (standard deviation) and emission (EM) reported as a range of the 2 models. md represents missing data.

Date	CO _{2SW} μM	CO _{2BW} μM	CO _{2EM} mmol m ⁻² d ⁻¹	CH _{4SW} μM	CH _{4BW} μM	CH _{4EM} mmol m ⁻² d ⁻¹
1 Jun 2016	81 (23)	79 (0)	42.3–73.9	0.35 (0.12)	0.25 (0.01)	0.17–0.30
14 June 2016	89 (14)	122 (11)	48.9–103.7	0.23 (0.08)	0.22 (0.07)	0.10–0.21
28 June 2016	69 (3)	172 (59)	38.0–79.4	0.56 (0.02)	0.61 (0.31)	0.35–0.73
12 July 2016	62 (6)	158 (112)	37.5–79.8	0.29 (0.04)	0.47 (0.40)	0.17–0.36
26 July 2016	47 (8)	215 (49)	25.0–56.5	0.25 (0.03)	0.19 (0.04)	0.14–0.31
9 August 2016	76 (4)	260 (89)	36.8–77.9	0.48 (0.07)	0.34 (0.15)	0.24–0.52
23 August 2016	94 (6)	182 (144)	51.1–111.4	0.45 (0.07)	0.62 (0.46)	0.24–0.53
6 September 2016	109 (2)	157 (135)	49.0–108.7	0.48 (0.04)	0.84 (0.65)	0.21–0.48
20 September 2016	92 (8)	122 (2)	39.3–79.7	md	md	md
4 October 2016	88 (6)	89 (5)	28.0–58.5	0.27 (0.07)	0.23 (0.11)	0.08–0.18
18 October 2016	86 (2)	92 (3)	23.8–42.8	0.25 (0.11)	0.23 (0.11)	0.05–0.09

md = missing data.

to hydrological variables (Fig. 5), although CH₄:CO_{2SW} was also positively correlated to Temp_{Ant} and Strat_{Buoy}.

CO₂ and CH₄ emission

Variable CO₂ and CH₄ concentrations led to a wide range in CO_{2EM} (24–111 mmol m⁻² d⁻¹) and CH_{4EM} (0.1–0.7 mmol m⁻² d⁻¹) over the open water period. Emissions followed a similar temporal pattern as the corresponding gas concentration, with peak CO_{2EM} occurring in mid-June and at the end of August and peak CH_{4EM} occurring later in June (Table 1, Fig. 4). In general, during relatively windy periods (>2 m s⁻¹), high CO_{2EM} was associated with rapid changes in air temperature while high CH_{4EM} was associated with precipitation events (Supplemental Table S2). Following a complete water column mixing in early September, CO_{2EM} and CH_{4EM} both remained low.

Total CO_{2EM} and CH_{4EM} was variable over time. For example, total CO_{2EM} during the 2-week mixing period in August (9–23 Aug; 665–1448 mmol m⁻²) was 2 times the total CO_{2EM} during the 2-week stratification period in July (12–26 July; 325–735 mmol m⁻²). Similarly, total CH_{4EM} during the rainy 2-week period at the end of June (14–28 June; 4.5–9.5 mmol m⁻²) was more than double the total CH_{4EM} during the following dry 2-week period (28 June to 12 July; 2.2–4.7 mmol m⁻²). Incorporating variation in surface water gas concentrations increased the total CO₂ and CH₄ emissions for the study period by 4% and 13%, respectively, when compared to the conventional method using only the gas concentration at the central point in the lake (i.e., L_{Central}).

Discussion

This study suggests that the drivers of CO₂ and CH₄ concentrations in the lake vary in space and time (Fig. 6), with important implications for whole-lake C budgets and

annual emission estimates. Given that the studied lake is small and partially surrounded by a mire complex, we predicted that CO₂ and CH₄ concentrations would be higher at the nearshore L_{Mire} than at other lake sites. Although water entering the lake from the mire subbasin (i.e., C_{Mire}) had higher CO₂ and CH₄ concentrations compared to C_{Forest} (Fig. 2g–h), only CH₄ (i.e., not CO₂) was elevated at the nearshore L_{Mire} site (Fig. 2b, e). Furthermore, our prediction that hydrology (a proxy for catchment inputs) would be a more important driver of CO₂ and CH₄ concentration than temperature (proxy for internal production and consumption) and lake stratification (proxy for vertical within lake connectivity) was mainly true for CH₄ (Table 2, Fig. 6). Overall, these observations highlight some inherent differences between spatial and temporal patterns in CO₂ and CH₄.

Interestingly, and contradicting our prediction, we found C_{Mire} groundwater to be CO₂-rich, whereas there was no clear influence of this input on CO₂ concentrations at the nearshore L_{Mire} site. In fact, we observed no significant differences in CO_{2SW} among the 5 surface-water sampling locations (Fig. 2a). Homogeneity in surface water CO₂ has previously been shown to result from a tilt in the thermocline caused by wind upwelling (Natchimuthu et al. 2017). However, upwelling can also drive heterogeneity in surface water CO₂ (Natchimuthu et al. 2017), and thus our observed homogeneity cannot solely be explained by wind induced upwelling events. In addition, specific discharge during summer can be much higher from mires than forest soils in this landscape (Karlsen et al. 2016; Supplemental Fig. S2), and this could foster the mixing of mire-derived, CO₂-rich waters throughout the lake. Finally, higher bioavailability of forest- versus mire-derived DOM pools (Kothawala et al. 2015) can lead to greater C mineralization in their draining waters (Berggren et al. 2007). Consequently, enhanced mineralization in the forested subbasin of Lake Stortjärn could mask the influence of CO₂-rich water entering the mire subbasin. To evaluate these

Table 2. Kendall's τ rank correlation coefficient for the association between gas concentration and antecedent temperature and precipitation (Temp_{Ant} , Prec_{Ant}), lake outlet discharge (Q_{Out}), and lake stratification strength ($\text{Strat}_{\text{Buoy}}$).

	$\text{CO}_{2\text{SW}}$	$\text{CO}_{2\text{BW}}$	$\text{CH}_{4\text{SW}}$	$\text{CH}_{4\text{BW}}$	$\text{CH}_4:\text{CO}_{2\text{SW}}$	$\text{CH}_4:\text{CO}_{2\text{BW}}$
Temp_{Ant}	-0.48****	0.54****	ns	ns	0.54****	ns
Prec_{Ant}	-0.22*	0.43***	0.48****	ns	0.63****	ns
Q_{Out}	ns	ns	0.52****	0.34**	0.24*	0.39***
$\text{Strat}_{\text{Buoy}}$	-0.45****	0.21*	ns	ns	0.25*	ns

Significance level: *0.05, **0.01, ***0.001, ****0.0001 and not significant (ns).

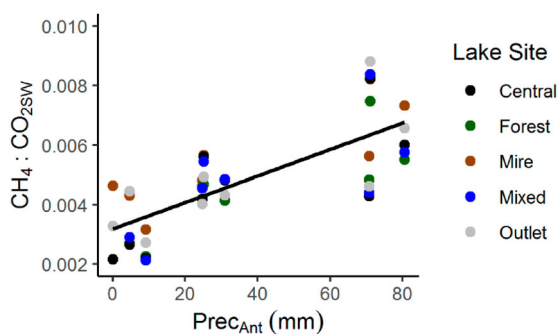
alternative mechanisms, studies investigating spatial variability in C source and composition as well as the fate of the within-lake DOM pool are warranted.

Although we did not observe a significant spatial variation in $\text{CO}_{2\text{SW}}$, we found that $\text{CO}_{2\text{BW}}$ was higher at the L_{Central} site than all other nearshore sites (Fig. 2d). This pattern has previously been reported for surface water CO_2 concentrations (Schilder et al. 2013, Natchimuthu et al. 2017) but has yet to be fully recognized for bottom water CO_2 . Over the sampling period, small-scale mixing events prevented nearshore sites from developing a consistent stratification, whereas in the deeper pelagic L_{Central} site, stratification was more persistent (Supplemental Fig. S1) and resulted in a bottom water O_2 reduction and accumulation of CO_2 (Supplemental Fig. S3). Additionally, although aerobic CH_4 oxidation has been observed throughout the water column, it is often most extensive at the aerobic–anaerobic interface (Bastviken et al. 2004) and thus may have been an additional source of CO_2 at the L_{Central} site. This mechanism is supported by relatively low $\text{CH}_{4\text{BW}}$ at the L_{Central} site (Fig. 2d). Other factors that may have contributed to low $\text{CH}_{4\text{BW}}$ at the L_{Central} site include cool sediment temperatures, low organic carbon quality in sediments as a result of low overall productivity, and the presence of more energetically favorable alternative electron acceptors (L. S. E. Praetzel and others, unpubl). At nearshore sites, CO_2 production was likely still high, but constant loss of CO_2 to the atmosphere resulted in lower $\text{CO}_{2\text{BW}}$.

CO_2 concentrations in surface and bottom waters also showed different temporal dynamics over time. Overall,

temporal patterns in CO_2 seemed to emerge from multiple drivers, but these influenced surface and bottom waters in opposite directions. For example, $\text{CO}_{2\text{SW}}$ declined with Temp_{Ant} , which could reflect enhanced photosynthesis (CO_2 uptake) during sunny, warm days (Natchimuthu et al. 2014). Such a mechanism could explain why temperature was only negatively related to $\text{CO}_{2\text{SW}}$, but not $\text{CO}_{2\text{BW}}$, because the photic zone, and thus primary production, is limited to the top meter of Lake Stortjärn (Denfeld et al. 2018). Furthermore, the negative relationship with stratification strength and $\text{CO}_{2\text{SW}}$ may reflect the upwelling of CO_2 -rich waters from depth (MacIntyre et al. 1999). By comparison, CO_2 in deep bottom waters showed a contrasting pattern, with accumulation during times of stable hypolimnion stratification and depletion during mixing. A direct link between CO_2 and precipitation and hydrological inputs was not as apparent. In fact, $\text{CO}_{2\text{SW}}$ was negatively related to precipitation, which is surprising considering that many studies have found the opposite (Rantakari and Kortelainen 2005, Ojala et al. 2011, Vachon and del Giorgio 2014). Yet we did observe that $\text{CO}_{2\text{BW}}$ increased with Prec_{Ant} , suggesting that rain-induced waters to some extent elevated within-lake CO_2 concentrations and/or O_2 concentrations in deeper waters.

Unlike CO_2 concentrations, the spatial response of CH_4 was similar in surface and bottom waters; CH_4 concentrations were elevated at nearshore sites, particularly near the mire complex. The proximity to the mire complex explained some of the spatial heterogeneity in CH_4 among littoral zones with especially high $\text{CH}_4:\text{CO}_2$ near the shore (Fig. 5). In addition to CH_4 -rich mire water entering the lake, other well-known processes such as elevated diffusion and ebullition in warm littoral lake sediments (Bastviken et al. 2008, DelSontro et al. 2016) and presence of macrophytes (Juutinen et al. 2003, Wang et al. 2006) likely elevated littoral CH_4 concentrations. Although mires in this region and elsewhere are known hotspots for CH_4 production and emission (Din-smore et al. 2010, Campeau et al. 2017), little research has linked their importance to CH_4 variability in lakes. Because mires are abundant in northern Sweden (Nilsson et al. 2001) and frequently co-occur with lakes, they likely represent overlooked conduits for CH_4 supply to lentic systems in this region.

**Figure 5.** Relationship between the ratio of CH_4 to CO_2 in lake surface waters ($\text{CH}_4:\text{CO}_{2\text{SW}}$) and 2-week antecedent precipitation (Prec_{Ant}).

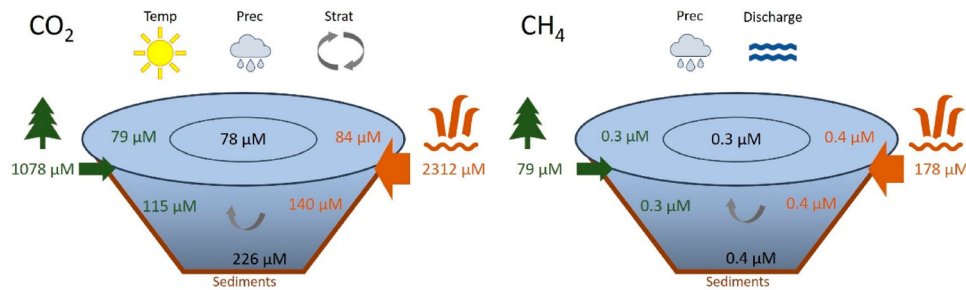


Figure 6. Conceptual within-lake spatial CO_2 and CH_4 patterns in a small boreal lake. Average CO_2 and CH_4 concentrations in surface and bottom waters of the lake center (black), forest nearshore (green), and mire nearshore (brown) sites. The relative concentration of CO_2 and CH_4 inputs from catchment waters draining forest/mineral soils (green arrow) and a mire complex (brown arrow) are represented by arrow size specific to each C gas. Spatial concentration patterns are driven by temporal changes in precipitation and discharge (proxies for hydrological loading of mire and forest catchment inputs), temperature (proxy for internal production and consumption rates), and lake stratification (proxy for vertical lake connectivity). Only temporal drivers with a significant correlation to the gas concentration are displayed (Table 2).

Although hydrologic connections to the adjacent mire seemed to dominate spatial patterns of CH_4 , inputs from forest soil waters also likely influenced the temporal variability in this gas. During wet periods, the $\text{CH}_4:\text{CO}_2\text{SW}$ ratio was elevated across all sampling sites (Fig. 5), indicating that CH_4 responded more strongly to precipitation than CO_2 , and that rainfall increased the lateral transport of riparian water rich in CH_4 from both forest soils and the mire complex (e.g., Lupon et al. 2019). Additionally, hydrological inputs of dissolved organic carbon (DOC) from catchment soils could further promote CH_4 production under anaerobic conditions. A study measuring DOC input to streams in this same landscape showed that mire inputs tend to dominate such inputs during low flow, but that forest soil sources become increasingly important as discharge increases (Laudon et al. 2011). Importantly, increased CH_4SW at the L_{Central} and L_{Outlet} site during precipitation events suggests that water from the catchment was largely transported horizontally across the lake as well as downstream. Thus, precipitation events likely contributed to CH_4 dynamics in both littoral and pelagic waters of the lake, through enhanced lateral transport of riparian C inputs and subsequent horizontal transport across the lake.

Interestingly, CH_4BW was correlated with discharge but not precipitation, indicating that the response to rainfall events differed in the surface versus bottom of the lake. Although stream discharge and precipitation are known to be positively related (Rasilo et al. 2012), the retention of rainwater within the surrounding catchment and lake caused a delayed response between lake outlet discharge and precipitation inputs (Supplemental Fig. S1), and thus a corresponding delayed response for CH_4BW . This delayed response could result from CH_4 -rich catchment water either entering the lake surface and being

transported vertically to greater depth (Hofmann 2013) or directly entering bottom waters via deeper preferential flow path through mires (Sponseller et al. 2018). Both explanations are plausible because an increase in CH_4BW lagged the observed increase in CH_4SW (Fig. 3b), particularly at the L_{Mire} site. Accordingly, it is evident that the response of within-lake CH_4 to precipitation events is variable in time and space, and future studies that address hydrological travel times and mixing of CH_4 from lake inflows to outflows are needed to better understand the mechanisms driving this variability.

The timing of peak emission differed between CO_2 and CH_4 (Fig. 4). The highest CH_4EM was observed in late June while the highest CO_2EM occurred in mid-June and late August, the latter corresponding to autumn turnover when high emissions are common in small boreal lakes (Riera et al. 1999, López Bellido et al. 2009). In Lake Stortjärn, ice-off at the end of May is typically followed by high CO_2 and CH_4 emissions during spring melt (Denfeld et al. 2018). Thus, the high C gases concentration and associated emission in June could be from C gases accumulated over the winter, which may be the case for CO_2 because in early June the lake was mixed with relatively high CO_2 concentrations and the lake outlet discharge was high from spring snow and ice melt (Supplemental Fig. S2b). However, highest CH_4EM in late June was likely not from winter C accumulation because the lake was thermally stratified (Fig. 4). Rather, the high CH_4EM more likely resulted from increased precipitation (Supplemental Table S2), which has been reported for both CO_2 and CH_4 emissions in other boreal lakes (Ojala et al. 2011, Rasilo et al. 2012).

Given that CO_2 and CH_4 emissions in our small boreal lake were sensitive to changes in precipitation and temperature (in the case of CO_2), we suggest that

efforts to quantify annual emissions need to incorporate the responses of C gases emission to short-term weather events. In this context, we found that the main driver of temporal emission differed between C gases, with hydrological changes most important for CH₄ and temperature and lake stratification most important for CO₂. Indeed, we found that not accounting for temporal variation in C gases emission estimates was more problematic than not accounting for spatial variation. Similarly, in other small boreal lakes, temporal variation in CO₂ emission was found to be greater than spatial variation (Natchimuthu et al. 2017, Klaus et al. 2019). Nevertheless, spatial variation was still important for CH₄ emissions from the lake and likely reflects the sporadic behavior of CH₄ (Bastviken et al. 2004, Natchimuthu et al. 2016) and, in particular for our lake, high CH₄ inputs from the mire complex. Taken together, when making annual C gas emission estimates from small lakes, temporal variation may be most important to consider, but the spatial variation of CH₄ should not be overlooked.

This study highlights that mixed land cover types (forest and mires) in small boreal lake catchments, a defining feature of the Swedish landscape (Kothawala et al. 2014), have varying effects on CO₂ and CH₄ concentrations. Most notably, the mire complex bordering the lake shore had a strong influence on within-lake CH₄ concentrations. The relative importance of land cover types on within-lake C gases variability may play a more important role in small lakes compared to large lakes because the relative importance of hydrological loading tends to be greater for lakes with shorter residence times (Vachon et al. 2017a). This scenario may also be true for the observed importance of precipitation on C gases variability, although precipitation has been shown to increase CO₂ concentrations in larger lakes as well (Rantakari and Kortelainen 2005, Ojala et al. 2011). Nevertheless, because the variability of precipitation events is predicted to increase in the boreal region (Teutschbein et al. 2018), knowledge of the controls on lateral fluxes from mixed landscapes to lakes is key to fully understanding the whole-lake C budget and how hydrologically induced C sourced to lakes may be altered with climate change.

Acknowledgements

We thank Peder Blomkvist, Kim Lindgren, Johannes Tiwari, Viktor Sjöblom, Abdulmajid Mahomoud, Ida Taberman, Åsa Boily, Ishi Buffan, Katharina Konradsson, and Ola Olofsson for their field, lab and/or database assistance. This work benefited from the Swedish Infrastructure for Ecosystem Science (SITES) and the Global Lake Ecological Observatory Network (GLEON) networks. Blaize Denfeld was financed by the Kempe Foundation. Anna Lupon was financed by the

Kempe Foundation and a Beatriu de Pinós (BP-2018-00082) grant. All data can either be accessed via www.slu.se/Krycklan or by request to authors.

Disclosure statement

No potential conflict of interest was reported by the author(s).

Funding

This work was supported by Kempestiftelserna; Beatriu de Pinós: [Grant Number BP-2018-00082]. This work was supported by Kempestiftelserna; Beatriu de Pinós fellowship programme funded by the Secretary of Universities and Research (Government of Catalonia) and is co-funded by the Marie Skłodowska-Curie grant agreement No 801370.

ORCID

Blaize A. Denfeld  <http://orcid.org/0000-0003-4391-7399>

References

- Åberg J, Jansson M, Jonsson A. 2010. Importance of water temperature and thermal stratification dynamics for temporal variation of surface water CO₂ in a boreal lake. *J Geophys Res Biogeosci.* 115:G02024.
- Bartosiewicz M, Laurion I, MacIntyre S. 2015. Greenhouse gas emission and storage in a small shallow lake. *Hydrobiologia.* 757:101–115.
- Bastviken D, Cole J, Pace M, Tranvik L. 2004. Methane emissions from lakes: dependence of lake characteristics, two regional assessments, and a global estimate. *Global Biogeochem Cy.* 18:GB4009.
- Bastviken D, Cole JJ, Pace ML, Van de Bogert MC. 2008. Fates of methane from different lake habitats: connecting whole-lake budgets and CH₄ emissions. *J Geophys Res.* 113:G02024.
- Bastviken D, Tranvik LJ, Downing JA, Crill PM, Enrich-Prast A. 2011. Freshwater methane emissions offset the continental carbon sink. *Science.* 331:50.
- Berggren M, Laudon H, Jansson M. 2007. Landscape regulation of bacterial growth efficiency in boreal freshwaters. *Global Biogeochem Cy.* 21:GB4002.
- Campeau A, Bishop KH, Billett MF, Garnett MH, Laudon H, Leach JA, Nilsson MB, Öquist MG, Wallin MB. 2017. Aquatic export of young dissolved and gaseous carbon from a pristine boreal fen: implications for peat carbon stock stability. *Global Chang Biol.* 23:5523–5536.
- Cole JJ, Caraco NF. 1998. Atmospheric exchange of carbon dioxide in a low-wind oligotrophic lake measured by the addition of SF₆. *Limnol Oceanogr.* 43:647–656.
- Cole JJ, Prairie YT, Caraco NF, McDowell WH, Tranvik LJ, Striegl RG, Duarte CM, Kortelainen P, Downing JA, Middelburg JJ, et al. 2007. Plumbing the global carbon cycle: integrating inland waters into the terrestrial carbon budget. *Ecosystems.* 10:171–184.
- Crusius J, Wanninkhof R. 2003. Gas transfer velocities measured at low wind speed over a lake. *Limnol Oceanogr.* 48:1010–1017.

- DelSontro T, Boutet L, St-Pierre A, del Giorgio PA, Prairie YT. 2016. Methane ebullition and diffusion from northern ponds and lakes regulated by the interaction between temperature and system productivity. *Limnol Oceanogr.* 61:62–77.
- Denfeld BD, Klaus M, Laudon H, Sponseller RA, Karlsson J. 2018. Carbon dioxide and methane dynamics in a small boreal lake during winter and spring melt-events. *J Geophys Res-Biogeosci.* 123(8):2527–2540.
- Dinsmore KJ, Billett MF, Skiba UM, Rees RM, Drewer J, Helfter C. 2010. Role of the aquatic pathway in the carbon and greenhouse gas budgets of a peatland catchment. *Global Change Biol.* 16:2750–2762.
- Encinas Fernández J, Peeters F, Hofmann H. 2016. On the methane paradox: Transport from shallow water zones rather than in situ methanogenesis is the major source of CH₄ in the open surface water of lakes. *J Geophys Res Biogeosci.* 121:2717–2726.
- Gelbrecht J, Fait M, Dittrich M, Steinberg C. 1998. Use of GC and equilibrium calculations of CO₂ saturation index to indicate whether freshwater bodies in north-eastern Germany are net sources or sinks for atmospheric CO₂. *Fresen J Anal Chem.* 361:47–53.
- Hartmann DL, Klein Tank AMG, Rusticucci M, Alexander LV, Brönnimann S, Charabi Y, Dentener FJ, Dlugokencky EJ, Easterling DR, Kaplan A, et al. 2013. Observations: atmosphere and surface. In: Stocker TF, Qin D, Plattner GK, Tignor M, Allen SK, Boschung J, Nauels A, Xia Y, Bex V, Midgley PM, editors. *Climate change 2013: the physical science basis. Contribution of Working Group I to the fifth assessment report of the Intergovernmental Panel on Climate Change.* Cambridge (UK) and New York (NY): Cambridge University Press; p. 208–220.
- Heiskanen JJ, Mammarella I, Haapanala S, Pumpanen J, Vesala T, Macintyre S, Ojala A. 2014. Effects of cooling and internal wave motions on gas transfer coefficients in a boreal lake. *Tellus B.* 66:22827.
- Hofmann H. 2013. Spatiotemporal distribution patterns of dissolved methane in lakes: How accurate are the current estimations of the diffusive flux path? *Geophys Res Lett.* 40:2779–2784.
- Jähne B, Münnich KO, Böisinger R, Dutzi A, Huber W, Libner P. 1987. On the parameters influencing air–water gas exchange. *J Geophys Res.* 92:1937–1949.
- Jennings E, Jones S, Arvola L, Staehr PA, Gaiser E, Jones ID, Weathers KC, Weyhenmeyer GA, Chiu CY, De Eyto E. 2012. Effects of weather-related episodic events in lakes: an analysis based on high-frequency data. *Freshwater Biol.* 57:589–601.
- Juutinen S, Alm J, Larmola T, Huttunen JT, Morero M, Martikainen PJ, Silvola J. 2003. Major implication of the littoral zone for methane release from boreal lakes. *Global Biogeochem Cy.* 17:1117.
- Juutinen S, Rantakari M, Kortelainen P, Huttunen JT, Larmola T, Alm J, Silvola J, Martikainen PJ. 2009. Methane dynamics in different boreal lake types. *Biogeosciences.* 6:209–223.
- Karlsen RH, Grabs T, Bishop K, Buffam I, Laudon H, Seibert J. 2016. Landscape controls on spatiotemporal discharge variability in a boreal catchment. *Water Resour Res.* 52:6541–6556.
- Karlsson J, Giesler R, Persson J, Lundin E. 2013. High emission of carbon dioxide and methane during ice thaw in high latitude lakes. *Geophys Res Lett.* 40:1123–1127.
- Klaus M, Seekell D, Lidberg W, Karlsson J. 2019. Evaluations of climate and land management effects on lake carbon cycling need to account temporal variability in CO₂ concentration. *Global Biogeochem Cy.* 33:243–265.
- Kortelainen P, Rantakari M, Huttunen JT, Mattsson T, Alm J, Juutinen S, Larmola T, Silvola J, Martikainen PJ. 2006. Sediment respiration and lake trophic state are important predictors of large CO₂ evasion from small boreal lakes. *Global Change Biol.* 12:1554–1567.
- Kothawala DN, Ji X, Laudon H, Ågren AM, Futter MN, Köhler SJ, Tranvik LJ. 2015. The relative influence of land cover, hydrology, and in-stream processing on the composition of dissolved organic matter in boreal streams. *J Geophys Res-Biogeosci.* 120:1491–1505.
- Kothawala DN, Stedmon CA, Müller RA, Weyhenmeyer GA, Köhler SJ, Tranvik LJ. 2014. Controls of dissolved organic matter quality: evidence from a large-scale boreal lake survey. *Global Change Biol.* 20:1101–1114.
- Laudon H, Berggren M, Ågren A, Buffam I, Bishop K, Grabs T, Jansson M, Köhler S. 2011. Patterns and dynamics of dissolved organic carbon (DOC) in boreal streams: the role of processes, connectivity, and scaling. *Ecosystems.* 14:880–893.
- Laudon H, Taberman I, Ågren A, Futter M, Ottosson-Löfvenius M, Bishop K. 2013. The Krycklan catchment study – a flagship infrastructure for hydrology, biogeochemistry, and climate research in the boreal landscape. *Water Resour Res.* 49:7154–7158.
- Leach JA, Larsson A, Wallin MB, Nilsson MB, Laudon H. 2016. Twelve year interannual and seasonal variability of stream carbon export from a boreal peatland catchment. *J Geophys Res-Biogeosci.* 121:1851–1866.
- Loken LC, Crawford JT, Schramm PJ, Stadler P, Desai AR, Stanley EH. 2019. Large spatial and temporal variability of carbon dioxide and methane in a eutrophic lake. *J Geophys Res-Biogeosci.* 124:2248–2266.
- López Bellido JL, Tulonen T, Kankaala P, Ojala A. 2009. CO₂ and CH₄ fluxes during spring and autumn mixing periods in a boreal lake (Pääjärvi, southern Finland). *J Geophys Res-Biogeosci.* 114:G04007.
- Lupon A, Denfeld BA, Laudon H, Leach J, Karlsson J, Sponseller RA. 2019. Groundwater inflows control patterns and sources of greenhouse gas emissions from streams. *Limnol Oceanogr.* 64:1545–1557.
- MacIntyre S, Flynn KM, Jellison R, Romero J. 1999. Boundary mixing and nutrient fluxes in Mono Lake, California. *Limnol Oceanogr.* 44:512–529.
- Murase J, Sakai Y, Sugimoto A, Okubo K, Sakamoto M. 2003. Sources of dissolved methane in Lake Biwa. *Limnology.* 4:91–99.
- Natchimuthu S, Panneer Selvam B, Bastviken D. 2014. Influence of weather variables on methane and carbon dioxide flux from a shallow pond. *Biogeochemistry.* 119:403–413.
- Natchimuthu S, Sundgren I, Gålfalk M, Klemedtsson L, Crill P, Danielsson Å, Bastviken D. 2016. Spatiotemporal variability of lake CH₄ fluxes and its influence on annual whole lake emission estimates. *Limnol Oceanogr.* 61:13–26.
- Natchimuthu S, Sundgren I, Gålfalk M, Klemedtsson L, Bastviken D. 2017. Spatiotemporal variability of lake

- pCO₂ and CO₂ fluxes in a hemiboreal catchment. *J Geophys Res-Biogeosci.* 122:30–49.
- Nilsson M, Mikkelä C, Sundh I, Granberg G, Svensson BH, Ranney B. 2001. Methane emission from Swedish mires: national and regional budgets and dependence on mire vegetation. *J Geophys Res-Atmos.* 106:20847–20860.
- Ojala A, Bellido JL, Tulonen T, Kankaala P, Huotari J. 2011. Carbon gas fluxes from a brown-water and a clear-water lake in the boreal zone during a summer with extreme rain events. *Limnol Oceanogr.* 56:61–76.
- Rantakari M, Kortelainen P. 2005. Interannual variation and climatic regulation of the CO₂ emission from large boreal lakes. *Global Change Biol.* 11:1368–1380.
- Rasilto T, Ojala A, Huotari J, Pumpanen J. 2012. Rain induced changes in carbon dioxide concentrations in the soil–lake–brook continuum of a boreal forested catchment. *Vadose Zone J.* 11:2.
- Read JS, Hamilton DP, Jones ID, Muraoka K, Winslow LA, Kroiss R, Wu CH, Gaiser E. 2011. Derivation of lake mixing and stratification indices from high-resolution lake buoy data. *Environ Model Softw.* 26:1325–1336.
- Riera JL, Schindler JE, Kratz TK. 1999. Seasonal dynamics of carbon dioxide and methane in two clear-water lakes and two bog lakes in northern Wisconsin, USA. *Can J Fish Aquat Sci.* 56:265–274.
- Schilder J, Bastviken D, Van Hardenbroek M, Kankaala P, Rinta P, Stötter T, Heiri O. 2013. Spatial heterogeneity and lake morphology affect diffusive greenhouse gas emission estimates of lakes. *Geophys Res Lett.* 40:5752–5756.
- Sponseller RA, Blackburn M, Nilsson MB, Laudon H. 2018. Headwater mires constitute a major source of nitrogen (N) to surface waters in the boreal landscape. *Ecosystems.* 21:31–44.
- Staehr PA, Christensen JPA, Batt RD, Read JS. 2012. Ecosystem metabolism in a stratified lake. *Limnol Oceanogr.* 57:1317–1330.
- Stanley EH, Casson NJ, Christel ST, Crawford JT, Loken LC, Oliver SK. 2016. The ecology of methane in streams and rivers: patterns, controls, and the global significance. *Ecol Monogr.* 86:146–171.
- Striegl RG, Michmerhuizen CM. 1998. Hydrologic influence on methane and carbon dioxide dynamics at two north-central Minnesota lakes. *Limnol Oceanogr.* 43:1519–1529.
- Teutschbein C, Grabs T, Laudon H, Karlsen RH, Bishop K. 2018. Simulating streamflow in ungauged basins under a changing climate: the importance of landscape characteristics. *J Hydrol.* 561:160–178.
- Tranvik LJ, Downing JA, Cotner JB, Loiselle SA, Striegl RG, Ballatore TJ, Dillon P, Finlay K, Fortino K, Knoll LB, et al. 2009. Lakes and reservoirs as regulators of carbon cycling and climate. *Limnol Oceanogr.* 54:2298–2314.
- Vachon D, del Giorgio PA. 2014. Whole-lake CO₂ dynamics in response to storm events in two morphologically different lakes. *Ecosystems.* 17:1338–1353.
- Vachon D, Prairie YT, Guillemette F, Del Giorgio PA. 2017a. Modeling allochthonous dissolved organic carbon mineralization under variable hydrologic regimes in boreal lakes. *Ecosystems.* 20:781–795.
- Vachon D, Solomon C, del Giorgio P. 2017b. Reconstructing the seasonal dynamics and relative contribution of the major processes sustaining CO₂ emissions in northern lakes. *Limnol Oceanogr.* 62:706–722.
- Verpoorter C, Kutser T, Seekell DA, Tranvik LJ. 2014. A global inventory of lakes based on high-resolution satellite imagery. *Geophys Res Lett.* 41:6396–6402.
- Wallin M, Buffam I, Öquist M, Laudon H, Bishop K. 2010. Temporal and spatial variability of dissolved inorganic carbon in a boreal stream network: concentrations and downstream fluxes. *J Geophys Res Biogeosci.* 115:G02014.
- Wang H, Lu J, Wang W, Yang L, Yin C. 2006. Methane fluxes from the littoral zone of hypereutrophic Taihu Lake, China. *J Geophys Res-Atmos.* 111:1–8.
- Wanninkhof RH. 1992. Relationship between wind speed and gas exchange over the ocean. *J Geophys Res.* 97:7373–7382.
- Weiss R. 1974. Carbon dioxide in water and seawater: the solubility of a non-ideal gas. *Mar Chem.* 2:203–215.
- Wiesenburg DA, Guinasso NL. 1979. Equilibrium solubilities of methane, carbon monoxide, and hydrogen in water and sea water. *J Chem Eng Data.* 24:356–360.
- Winslow LA, Zwart JA, Batt RD, Dugan HA, Iestyn Woolway R, Corman JR, Hanson PC, Read JS. 2016. Lakemetabolizer: an R package for estimating lake metabolism from free-water oxygen using diverse statistical models. *Inland Waters.* 6:622–636.